Topology of the Singularities of 3-RPR Planar Parallel Robots

Christoforos Spartalis, Jose Capco

Topology of the Singularities of 3-RPR Planar Parallel Robots

Christoforos Spartalis, Jose Capco

University of Innsbruck, Technikerstrasse 13, 6020 Innsbruck, Austria

Abstract

Given a general 3-RPR planar parallel robot with linear platforms, it is proven that there are no singularity-free paths between non-symmetrical direct kinematics solutions. We provide an alternative proof of this. We also provide a proof that shows that there is a singularity-free path between two symmetrical solutions if an appropriate condition is satisfied. This condition will be automatically satisfied for exactly one symmetrical pair of solutions if there are four real solutions to the direct kinematics. The topology of the kinematic singularities of these robots is described. We prove that the complement of the singularity space in the domain of the kinematic map for such robots consists of three connected components. An analysis of special robots is also provided, i.e. when the anchor points of the moving platform and the fixed platform have the same cross-ratios. For this case we show that, the singularity-free space consists of four connected components, no direct kinematics solutions can be connected without crossing the singularity surface and that the absolute value of the determinant of the Jacobian of the kinematic map evaluates to the same number for any of the direct kinematics solutions. The topological analysis of the singularities of 3-RPR planar parallel robots with linear platforms is based on the fibers of the natural map $\mathrm{SE}(2) \to S^1$ restricted to the singularity set of the kinematic map, and this is a conic fibration. In fact this is also the case when one or both platforms are triangular. We use similar methodology as in the linear platforms case and show that in the case that one or both platforms are triangles the singularity-free space has two connected components. This result was already proven when both platforms are triangles but here a different approach is followed.

Keywords: 3-RPR parallel robots, singularities, inverse kinematics, conic fibrations

1. Introduction

Kinematic singularities have been an object of study with significant importance in robotics. A parallel robot in a singular pose loses its inherent infinite rigidity and has uncontrollable degrees of freedom (see [17]). Hence it might become shaky, harder to control and less predictable. Since these type of robots are used for pick-and-place tasks that require transporting heavy loads as well as for flight simulators such singular poses should be predicted and avoided throughout the tasks that these robots execute.

The most common and well studied spatial parallel robot is the Gough-Stewart platform, or 6-SPS parallel robot. Topics of interest include investigating singularities, self motions (see [12]) and the direct kinematics (see [19]). Current state of the art provides a rational parametrization of the singularity set for Gough-Stewart platforms for the general and biplanar case (see [4], [5]).

In this paper we are interested in the 3-RPR planar parallel robots with various architectural designs. These robots are the planar counterpart of the 6-SPS platform and are of interest mostly from a theoretical kinematic point of view since they are not common in applied robotics. They consist of a base-fixed platform and a moving one, that are connected via RPR legs. By an RPR

Email addresses: christoforos.spartalis@uibk.ac.at (Christoforos Spartalis), jose.capco@uibk.ac.at (Jose Capco)

leg we mean a linkage connecting passive revolute joints placed on the anchor points, three on each platform, that consist of an actuated prismatic joint allowing extension and contraction of the leg resulting in the motion of the moving platform.

Investigating the singularities of these robots amounts to computing the singularities of their respective kinematic maps. These are functions from SE(2) to $\mathbb{R}^3$ that map poses of the robot to the triplet consisting of the squared lengths of the legs. Hence we distinguish between different architectural designs since adding more design parameters would modify the kinematic map and consequently the singularities. In Section 2, we will deal with 3-RPR parallel robots with linear platforms and for simplicity we will often just call them *linear robots*. Section 3 deals with robots with triangle-line platforms, in short *hybrid robots*, and Section 4 deals with the most general case, i.e. robots for which both platforms are triangles, which will be called *triangular robots*.

Because of the simple structure of linear robots, one is able to fully analyse the topology of the singularities, in SE(2), of these mechanisms. We will therefore be very detailed in our analysis of the topology of the singularities in Section 2 in order to motivate a similar analysis (but with less detail) for the other sections. Despite the fact that the singularities of the three types of robots we deal with have different topologies, the main idea to analyse their topology remains the same (this is inspired by [16]): The natural projection to the orientation $\mathrm{SE}(2) \to S^1$ restricted to the kinematic singularity space Σ, is a map between quasi- projective varieties that is also a conic fibration over S^1 (see [7, 14]) and it suffices to understand the fibers of this map to understand the topology of Σ. There are good sources of literature for conic fibrations, however we cannot take full advantage of them as they mostly deal with complex projective varieties while we deal with real affine varieties. So in a sense, this work also provides an initial understanding of conic fibrations in real algebraic geometry and their application in robotics.

Some results known for linear robots are significantly simpler and perhaps somewhat surprisingly different from those of triangular robots. For instance, the number of real direct kinematics solutions for the robots with linear platforms can be proven to be at most four while this is six for the robots with triangular platforms (see Remark 2.2 or [16] or [17] Exercise 4.1). To investigate the direct kinematics one has to work with a system of polynomial equations. Some authors investigated similar systems numerically (e.g. [1, 20]), but here it is possible to follow an algebraic approach. Actually even more can be said about these linear robots and in this paper we will give an analysis of the topology of the singularity surface of this mechanism.

We provide a proof of a known fact that for a sufficiently general 3-RPR linear robot there are two distinct direct kinematics solutions that can be connected via a path that does not cross singularity. Such questions were asked for other planar and serial manipulators (e.g. [6] and [18] respectively) and is of interest to experts in robotics and kinematics [11]. Parallel (or serial) robots that have the property of switching between direct (equivalently inverse) kinematics solutions without crossing singularities are called *cuspidal* (see [21]).

In fact, more is known about 3-RPR linear robots. It was proven (in [16]) that there is a singularity-free path between two symmetrical direct kinematics solutions (i.e. pair of solutions for which the angles and heights of the moving platform have opposite signs) if these solutions lie in the exterior of their associated hyperbola. However because of a flaw of an argument in [16], it was wrongly believed that all symmetrical solutions can be connected. We provide a topological argument that shows that if the symmetrical solutions lie in the interior of their associated hyperbola then they cannot be connected via a singularity-free path (see Remark 2.7).

There is a subtle point in our proof, it provides geometric and topological insights to the kinematic singularity surface in SE(2). We also show a new result for linear robots, namely that the singularity-free space of a sufficiently general 3-RPR robot consists of three connected components and then provide an alternative proof that non-symmetrical solutions cannot be connected without crossing singularities. We also study how the determinant of the Jacobian of the kinematic map evaluates at a point in any of these components. We provide explicit proof stating that the determinant of the Jacobian at non-symmetrical solutions evaluates to numbers with different signs (this is clear if the number of connected components of the singularity-free space is two, but we have three such components).

In subsection 2.2, we deal with special linear robots, namely those for which the linear platforms

have anchor points with the same cross-ratios. These robots differ from the general ones because no direct kinematics solutions can be connected without crossing singularity. The singularities of these robots have easy but interesting topological structures. For instance, the absolute value of the determinant of the Jacobian evaluates to the same number for any direct kinematics solution. Also the singularity-free space of these robots, in SE(2), consists of four connected components and all four direct kinematics solutions belong to distinct connected components.

In Section 3 the previous techniques on investigating the singularity surface are extended to hybrid robots, to prove that the singularity-free space in this case consists of only two connected components.

We investigate general 3-RPR robots (triangle-triangle) in Section 4. This mechanism has been studied in the past, e.g. [8, 13] investigate the direct kinematics problem and [9, 10] made analysis of the singularities. Our analysis led to a very simple proof of the fact that the number of connected components of the singularity-free space of this robot is two. This has been proven in [3, 9], however their method is different and requires more mathematical tools. The advantage of our method is its simplicity and it gives a complete description of the topology of the singularity surface (and not only the number of the connected components of its complement). We give a brief overview of how [9] and [3] prove their results before finally proving it using our analysis of the θ-sections (i.e. the fibers of the conic fibration). We did not need to look at a modified workspace to prove this result (as did in [3, 9]) and in our proof we can identify the singular points of the singularity surface of such mechanisms (these are pinch-points and have to do with θ-sections for which we have two intersecting lines rather than a smooth conic).

To complete, a brief analysis of the singularities of 3-RPR robots with similar, not reflected, triangular platforms is presented in subsection 4.2 (for some results in the reflected case see [22]). In this special case the number of connected components of the singularity-free space is four instead of two. This number remains the same even if we require that the triangles are congruent.

2. 3-RPR Linear Planar Platforms

Consider a 3-RPR planar parallel robot with linear platforms for which the anchor points are distinct. We will refer to it as *linear robot* for brevity throughout this section. We can without loss of generality, via scaling and change of zero-position, assume the following:

- The fixed platform lies on the x-axis.
- The moving platform at zero-position, i.e. when the transformation of the moving platform with respect to the fixed platform is identity, lies along the x-axis.
- The anchor points of the fixed platform are $(0,0), (1,0), (f_3,0)$ and at zero-position they are connected via an RPR leg to the anchor points $M_1 = (0,0)$, $M_2 = (m_2,0)$, $M_3 = (m_3,0)$ of the moving platform respectively, where $f_3, m_2, m_3 \in \mathbb{R}$.

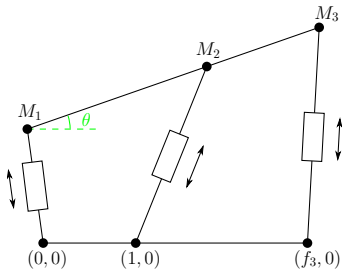

Figure 1: An illustration of a linear robot. The design parameters f_3, m_2, m_3 can take any value in $\mathbb{R}$ as long as the anchor points remain distinct.

We will now describe the kinematic map of this robot. For simplicity, we write an element $\sigma \in \mathrm{SE}(2)$ as a triple (θ, x, y) where θ determines the orientation and (x, y) the translation vector. We will also often, write c instead of $\cos\theta$ and s instead of $\sin\theta$.

Following the notations above, the kinematic map $F : \mathrm{SE}(2) \to \mathbb{R}^3$, of the robot is given by

$$F(\theta, x, y) := (x^2 + y^2, (m_2c - 1 + x)^2 + (m_2s + y)^2, (m_3c - f_3 + x)^2 + (m_3s + y)^2)$$

This map takes the transformation of the moving platform (centred at M_1) and maps it to the square of the length of each of the legs. We take the squared lengths because we would like to have a system of polynomial equations when solving the direct kinematics. Furthermore, the topology of the singular points of this function will be the same as that of the one that evaluates poses to lengths.

It is easy to compute the set of singularities of this map, it is given by:

$$\Sigma := \{(\theta, x, y) \in \mathrm{SE}(2) \ : \ D(c, s, x, y) = 0\}$$

where D is the determinant of the Jacobian of F and it is specifically the polynomial

$$-c(f_3m_2 - m_3)y^2 + s(f_3m_2 - m_3)xy + s^2m_2m_3(f_3 - 1)x - s(cm_2m_3(f_3 - 1) + f_3(m_2 - m_3))y$$

A linear robot will be called *general* when $f_3m_2 \neq m_3$, otherwise it will be called *special*. Suppose now that we are given squared leg length values $\boldsymbol{\ell} = (l_1, l_2, l_3) \in \mathbb{R}^3$. We investigate the *direct kinematics*, i.e. the fiber $F^{-1}(\boldsymbol{\ell})$. We have the following system of equations:

$$\begin{aligned} l_1 &= x^2 + y^2 \\ l_2 &= (m_2c - 1 + x)^2 + (m_2s + y)^2 \\ l_3 &= (m_3c - f_3 + x)^2 + (m_3s + y)^2 \end{aligned}$$

Remark 2.1. If there is a solution for which the two platforms are parallel ($\theta = 0$ or $\theta = \pi$), then $\boldsymbol{\ell}$ must lie in the union of two hyperplanes, i.e. $\boldsymbol{\ell} \in H_1 \cup H_2 \subseteq \mathbb{R}^3$. When this is not the case, we can get rid of the squares x^2 and y^2 by substituting the first equation in the last two and obtain a linear system in x and y. This linear system is independent when $f_3m_2 - m_3 \neq 0$ and $s \neq 0$.

Remark 2.2. For a general linear robot, we conclude that, if $\boldsymbol{\ell} \in \mathbb{R}^3 \backslash \{H_1 \cup H_2\}$ we can express x and y in terms of c and s and substitute these expressions in $l_1 = x^2 + y^2$ and, upon reduction modulo $c^2 + s^2 - 1$, obtain a univariate cubic polynomial $h(c) \in \mathbb{R}[c]$ (for detail description of h, see [2, 16]), where $c = \cos\theta$. This polynomial has the property that $h(1)$ and $h(-1)$ have the same signs, thus it will have at most two real roots in $(-1, 1)$. Hence, there are at most four distinct real solutions to the direct kinematics problem, since h is an even function of θ.

Additionally, in terms of θ, the direct kinematics solutions can be interpreted geometrically, as the intersection points of at most two vertical lines and the unit circle in the cs-plane. If the two lines coincide then this would imply that there exists a double real root of $h(c)$ in $(-1, 1)$. Thus by back substitution in the linear system for the direct kinematics two solutions with multiplicity two will arise, which is a singularity.

Remark 2.3. For a special linear robot, we conclude that, if $\boldsymbol{\ell} \in \mathbb{R}^3 \backslash \{H_1 \cup H_2\}$ we can solve for y in terms of x and c in the second equation. By substituting $y(x, c)$ in the third equation we get a linear polynomial in c. We check for a real root in (-1,1) and substitute it in $y(x, c)$. Finally we substitute $y(x)$ back into the first equation and solve a quadratic polynomial in x (see [2, 16]).

In both cases the solutions to the direct kinematics share the same geometric property, i.e. whenever (θ, x, y) is a solution, $(-\theta, x, -y)$ is a solution too. Such pair of solutions is called *symmetrical* (a term also used in [16]) because the moving platform at these positions and orientations are a reflection of each other with respect to the x-axis. Note also that $D(\theta, x, y) = D(-\theta, x, -y)$.

2.1. General Case

For the rest of this section we assume a general linear robot, i.e. $f_3 m_2 \neq m_3$. Firstly, we provide an alternative proof of a known result (see [16]).

Proposition 2.4. There exist two distinct elements $\sigma, \tau \in \mathrm{SE}(2) \setminus \Sigma$ such that

- $F(\sigma) = F(\tau)$
- There is a path $\gamma : [0,1] \to \mathrm{SE}(2)$ from σ to τ such that $\gamma([0,1]) \cap \Sigma = \emptyset$

Proof. We note that (see also [2])

$$D(\pm 1, 0, x, y) = \mp y^2 (f_3 m_2 - m_3)$$

So, for a general robot, $(0, x, y) \in \Sigma$ implies $y = 0$.

Let $\Delta_y(D)$ be the discriminant of D with respect to y. Then $\Delta_y(D)$ factors as

$$\Delta_y(D)(c, s, x) = g(x, c) s^2$$

where $g(x, c)$ is a quadratic polynomial in x and in c. For a general robot, the coefficient of x^2 in $g(x, c)$ does not vanish and is the positive value $(f_3 m_2 - m_3)^2$.

Let $\Delta_x(g)$ be the discriminant of g with respect to x. Then $\Delta_x(g)$ factors as

$$\Delta_x(g)(c) = p(m_2, m_3, f_3) c$$

where $p(m_2, m_3, f_3) = 16 f_3 m_2 m_3 (m_3 - m_2)(f_3 - 1)(f_3 m_2 - m_3)^2 \neq 0$, for a general robot.

Without loss of generality, assume that $p > 0$. Then for any $\theta \in (-\pi/2, \pi/2)$, $g(x, \cos\theta)$ will have two distinct roots in x and since the coefficient of x^2 is positive it attains negative values for any x between these two roots. Thus, we can find $x = \alpha$ such that $g(\alpha, 1) < 0$ and because g is continuous, there is a sufficiently small $\delta > 0$ such that $g(\alpha, \cos\theta) < 0$, for all $\theta \in (-\delta, \delta)$. If $p < 0$, we develop similar arguments in a neighbourhood around $\theta = \pi$ instead of $\theta = 0$.

Define the following path-connected set

$$X := (-\delta, \delta) \times \{\alpha\} \times \mathbb{R} \setminus \{(0, \alpha, 0)\}.$$

Note that by the previous analysis, any $(\theta, x, y) \in X$ is a regular point of the kinematic map. But since $F(\theta, x, y) = F(-\theta, x, -y)$, F restricted to X is not injective, i.e. there is a singularity-free path between two symmetrical direct kinematics solutions. □

Henceforth, without loss of generality assume that $p(m_2, m_3, f_3) > 0$. If we investigate the proof above we see that at the point $(\theta, x, y) = (0, \alpha, 0)$, where $\alpha \neq 0$, the set of real singularities is locally a line. This property of F was not directly revealed in [16].

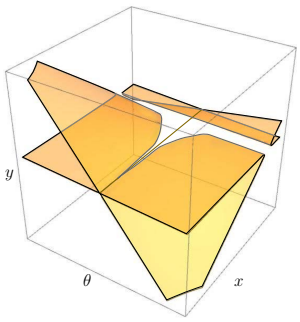

Figure 2: A local plot of Σ centred at $(\theta, x, y) = (0, 0, 0)$ for a robot with design parameters $f_3 = 2, m_2 = 3, m_3 = 5$. At $\theta = 0$ the singularities are locally a line, i.e. the x-axis.

Theorem 2.5. The complement of Σ consists of three connected components.

Proof. We will abuse our notations and write D evaluated at θ to mean $D(\cos\theta, \sin\theta, x, y)$. First we note that for a fixed $\theta \in [0, 2\pi)$, a section of Σ at this θ is a hyperbola (possibly degenerate). This is because the discriminant of the conic is

$$-(f_3 m_2 - m_3)^2 s^2$$

Moreover, the determinant of the Hessian of the quadratic form defining this conic equation is

$$f_3 m_2 m_3 (m_3 - m_2)(f_3 - 1)(f_3 m_2 - m_3) s^4$$

This implies that the hyperbola at a θ-section degenerates iff $\theta = 0$ or $\theta = \pi$. In fact, as our previous analysis shows, it degenerates into the double lines $y^2 = 0$. For a fixed θ, we will call the θ-section of Σ the hyperbola at θ, as illustrated in Figures 3 and 4.

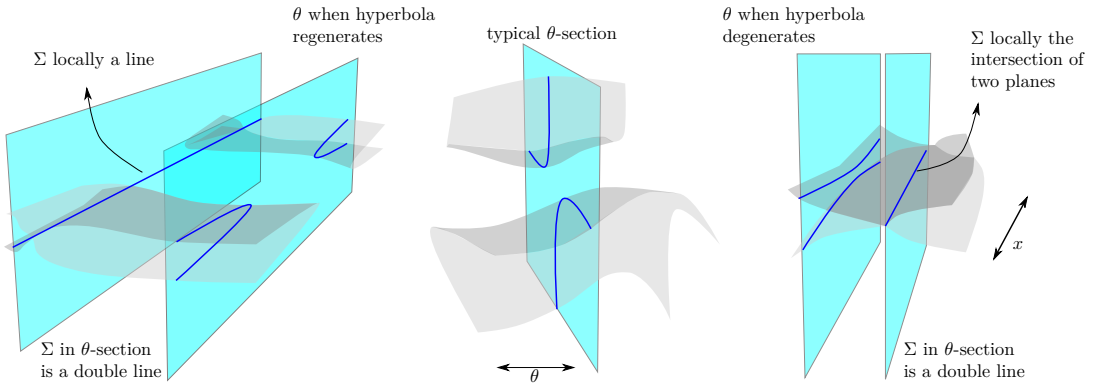

Figure 3: An artistic illustration of the θ-sections of Σ. At $\theta = 0$ (leftmost picture) and $\theta = \pi$ (rightmost picture) the hyperbola degenerates into a double line.

The slope of the principal axes of the hyperbola at θ is also determined by the entries of the Hessian of D. Specifically, the angle between the transverse axis of the hyperbola at θ and the x-axis is the half of θ. So the hyperbola rotates counter-clockwise as we change θ from 0 to 2π. Depending on the sign of $f_3 m_2 - m_3$, D evaluates any element in the $\theta = 0$ section to opposite sign than the ones in the $\theta = \pi$ section. Assume, without loss of generality, that D evaluates any element in the $\theta = 0$ section to non-positive values and any element in the $\theta = \pi$ section to non-negative values. Then as θ continuously changes from 0 to π the following things happen:

1. At $\theta = 0$, the transverse axis coincides with Σ.
2. When θ increases, the double line regenerates into two narrow branches of a hyperbola (see left image of Figure 3).
3. D evaluates to positive values in the interior[1] of the hyperbola $\forall\theta \in (0, \pi)$.
4. D evaluates to negative values in the exterior of the hyperbola $\forall\theta \in (0, \pi)$.
5. When θ is near π the branches become wider and are close to degenerate (see right image of Figure 3).
6. At $\theta = \pi$, the non-transverse axis coincides with Σ.

We can make similar observations when θ changes from π to 2π, where the hyperbola continues to rotate counter-clockwise but where the region for which D evaluates to positive values vanishes at $\theta = 2\pi$ (identifies with $\theta = 0$ in S^1). This behaviour of the hyperbola is illustrated in Figure 4.

Consider now a symmetrical pair $\sigma, \tau \in \mathrm{SE}(2)$ such that $D(\sigma) = D(\tau) < 0$. Then σ and τ are in the exterior of their associated hyperbolas. Without loss of generality assume that the orientation

[1] The interior of a conic consists of all the points of the plane that don't belong to any tangent of the conic.

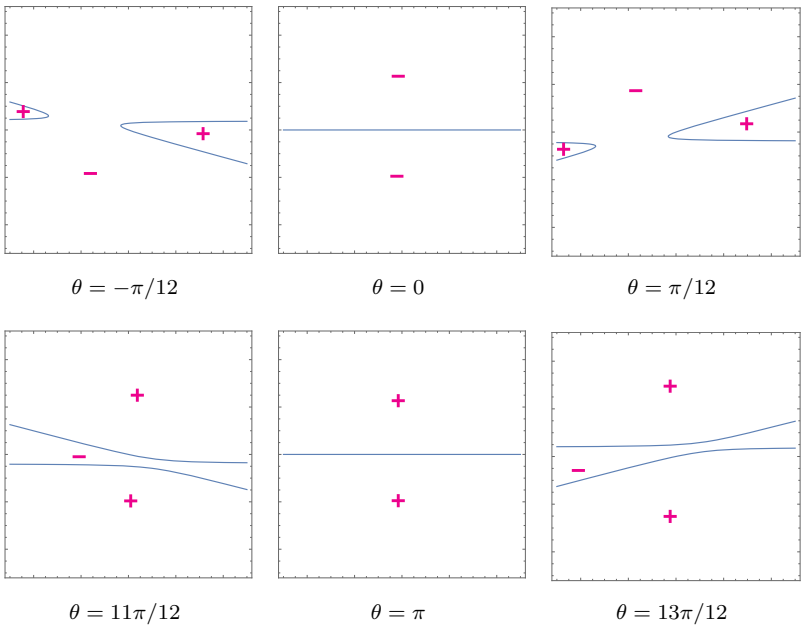

Figure 4: How D evaluates for different θ-sections

of σ is $\theta_0 \in (0, \pi)$. We can move from within the $\theta = \theta_0$ section to the opposite side of the transverse axis of the associated hyperbola without crossing Σ. We can then continuously follow the θ-sections with $\theta \in [-\theta_0, \theta_0]$ remaining on this 'opposite' side without crossing singularity (the hyperbola degenerates into double line at $\theta = 0$, but our path remains in the exterior of the associated hyperbolas without crossing singularity). This procedure is also described in [16] and takes the advantage of the fact that the exterior of a hyperbola is one connected component in the affine plane. With this we conclude that the 'exterior' of Σ is one connected component (i.e. points that lie in the exterior of the hyperbola at the θ-section that corresponds to their orientation).

Now take any $\theta \in (0, \pi) \cup (\pi, 2\pi)$, then the associated hyperbola has two connected components corresponding to the interior of the branches. We will show that these two 'interiors' cannot be connected. Continuously following the θ-section will lead us to conclude that possible connection only occurs when $\theta = \pi$ (at $\theta = 0$ the interior collapses and so we cannot traverse a path that meets $\theta = 0$). But, even at $\theta = \pi$ one cannot pass between the two interiors (at this point Σ looks locally like the intersection of two planes). In short, the two branches of the hyperbola at a $\theta \in (0, \pi) \cup (\pi, 2\pi)$ section correspond to two distinct connected components of $\mathrm{SE}(2) \backslash \Sigma$. Thus, we conclude that there are three connected components of $\mathrm{SE}(2) \backslash \Sigma$. □

In this proof more was shown. A symmetrical pair of solutions that lie in the exterior of their respective hyperbolas can be connected via a singularity-free path. If however, the symmetrical pair lie in the interior of their respective hyperbolas, then they cannot be connected via a singularity-free path. Also, F restricted to one of the connected components is two-to-one while F restricted to any of the other two components is one-to-one. Thus, we can state the following:

Corollary 2.6. There exists a singularity-free path between symmetrical direct kinematics solutions if and only if these solutions lie in the exterior of their respective hyperbolas.

Remark 2.7. We discovered a flaw to an argument in [16] where Merlet claimed that there is a singularity-free path between any symmetrical direct kinematics solutions. In his argument, Merlet does not consider the fact that the hyperbola degenerates at $\theta = 0$ and $\theta = \pi$ and suggests a path between a symmetrical pair of solutions in the interiors of Σ. The path that is suggested follows the θ-section continuously while remaining on the transverse axis and in the interior of

the associated hyperbola. However, at $\theta = 0$ (if $p < 0$, $\theta = \pi$), the interior vanishes (Σ is locally the intersection of two planes) and so the only possible path is when traversing $\theta = \pi$. It is still not possible to pass to the other branch even if the hyperbola branches completely 'open' (i.e. $\theta = \pi$) as seen in the proof of Theorem 2.5. So in [16], Merlet did not really accounted for the degeneration of the θ-sections of Σ.

Remark 2.8. At the end of Remark 2.2 we mentioned that symmetrical pairs of direct kinematics solutions can be geometrically represented as at most two vertical lines intersecting the unit circle in the cs-plane. Switching between two solutions would mean that the lines move horizontally along the circle until they intersect the circle in the original points. But now a reference point that we follow has switched places with another intersection point (see Figure 5 for an illustration of this motion). This geometric interpretation of a switch between solutions only in terms of θ provides arguments that prove the following results.

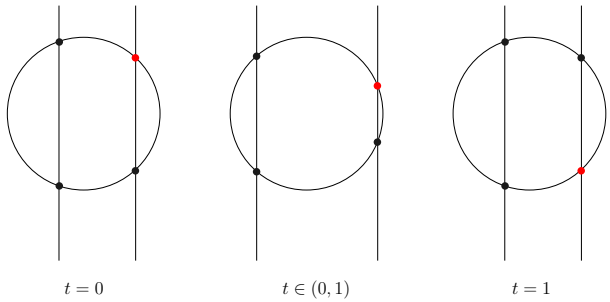

Figure 5: An illustration of the two lines representing the symmetrical pairs of solutions and the switching between two solutions of a symmetrical pair.

Proposition 2.9. Two non-symmetrical direct kinematics solutions cannot be connected without crossing singularities.

Proof. Suppose we have two distinct non-symmetrical and regular solutions. Consider the vertical lines and unit circle in the cs-plane as in Remark 2.8. Pick one of the intersections as a reference point. Assume that there is a path from a solution that corresponds to this reference point to a non-symmetrical solution. Switching between one solution of the direct kinematics to another means a horizontal motion of the two lines along the circle which would end when the lines intersect the circle exactly at the same points as they initially did. But now the reference point has moved to one of the other points (not the symmetrical one). The only way for this to happen is if the lines have eventually switched places and this happens only if they merge, which is a singularity, by Remark 2.2. □

Proposition 2.10. The determinant of the Jacobian evaluates two regular non-symmetrical direct kinematics solutions to opposite signs.

Proof. It is easy to check that symmetrical solutions evaluate to the same sign, since for any $(\theta, x, y) \in \mathrm{SE}(2)$, $D(c, s, x, y) = D(c, -s, x, -y)$. Assume that there exist two regular non-symmetrical solutions that evaluate to the same sign. Then all of the solutions would evaluate to the same sign, which would imply that all solutions lie either on the interior or the exterior of their respective hyperbolas. Then two non-symmetrical solutions could be connected without crossing singularities, for example the ones with positive θ, since the hyperbola rotates for $\theta \in (0, \pi)$ and continuously preserves the interior/exterior parts. But this contradicts Proposition 2.9. □

2.2. Special Case : Similar Platforms

As discussed in [16], solving the direct kinematics when $f_3 m_2 = m_3$, amounts to solving a second degree polynomial equation in x for a specific c and $y(x, c, s)$. Hence the solutions will

be of the form $\sigma_1 = (\theta, x_1, y_1)$, $\sigma_2 = (\theta, x_2, y_2)$ and $\tau_1 = (-\theta, x_1, -y_1)$, $\tau_2 = (-\theta, x_2, -y_2)$, when $\theta \neq 0$ or π.

Remark 2.11. By substituting $m_3 = f_3 m_2$ in D, we get

$$D(c, s, x, y) = f_3 m_2 (f_3 - 1)((1 - cm_2)y + sm_2 x)s$$

Thus we observe that, for $s = 0$, we get $D(\pm 1, 0, x, y) = 0, \forall x, y \in \mathbb{R}$. Hence, for any $(x, y) \in \mathbb{R}^2$, $(0, x, y) \in \Sigma$ and $(\pi, x, y) \in \Sigma$. Also, it should be noted that, when $\theta \neq 0$ and $\theta \neq \pi$ there will always be four distinct direct kinematics solutions for a regular value $\boldsymbol{\ell} = (l_1, l_2, l_3) \in \mathbb{R}^3$.

Proposition 2.12. If $\sigma_1 = (\theta, x_1, y_1)$ and $\sigma_2 = (\theta, x_2, y_2)$ are two solutions of the direct kinematics in the same θ-section, then $D(\sigma_1) = -D(\sigma_2)$.

Proof. By subtracting the first from the second equation of the direct kinematics we get,

$$2(cm_2 - 1)x + 2sm_2 y - 2cm_2 + m_2^2 + 1 + l_1 - l_2 = 0 \tag{1}$$

Since θ is the same in σ_1 and σ_2, they will belong in the same θ-section of SE(2), thus they will both satisfy equation (1), which can be rewritten, for some $\kappa \in \mathbb{R}$, as

$$(cm_2 - 1)x + sm_2 y + \kappa = 0 \tag{2}$$

Hence, (x_1, y_1) and (x_2, y_2) lie on a line in $xy-$plane with slope $\frac{1-cm_2}{sm_2}$. Additionally, they will be points on a circle with origin $(0, 0)$ and radius $\sqrt{l_1}$, since they both satisfy $x^2 + y^2 = l_1$.

On the other hand, the singularity set on this θ-section is the line

$$sm_2 x + (1 - cm_2)y = 0 \tag{3}$$

which passes through the origin of the xy-plane with slope $\frac{sm_2}{cm_2 - 1}$, hence it is a line perpendicular to the line defined by equation (2).

As a result, $(\frac{x_1+x_2}{2}, \frac{y_1+y_2}{2})$ will satisfy equation (3), which yields

$$(1 - cm_2)(y_1 + y_2) + sm_2(x_1 + x_2) = 0 \Leftrightarrow y_1(1 - cm_2) + x_1 sm_2 = -(y_2(1 - cm_2) + x_2 sm_2)$$

and thus $D(\theta, x_1, y_1) = -D(\theta, x_2, y_2)$. □

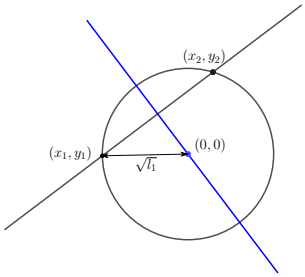

Figure 6: An example of the singularity line crossing the middle point of the chord between the two direct kinematics solutions (x_1, y_1) and (x_2, y_2) on the same θ-section.

Corollary 2.13. If $\sigma_1 = (\theta, x_1, y_1)$ and $\sigma_2 = (\theta, x_2, y_2)$ are two solutions of the direct kinematics in the same θ-section, then $(\theta, \lambda(x_1 + x_2), \lambda(y_1 + y_2)) \in \Sigma$ for any $\lambda \in \mathbb{R}$.

Corollary 2.14. All paths between direct kinematics solutions must cross singularities.

Proof. If $\sigma_1, \sigma_2, \tau_1, \tau_2$ are defined as in the beginning of this section, then for $i = 1, 2$ we get

$$D(\tau_i) = D(c, -s, x_i, -y_i) = D(c, s, x_i, y_i) = D(\sigma_i)$$

But since σ_i and τ_i, for $i = 1, 2$, belong in opposite signed θ-sections a path between them should involve crossing $\theta = 0$ or π which is a singularity. By Proposition 2.12, the determinant of the Jacobian evaluates solutions in the same θ-section to opposite signed values, hence they cannot be connected without crossing singularities. □

Corollary 2.15. The absolute value of the determinant of the Jacobian evaluates to the same number for all direct kinematics solutions.

Proof. From the previous results, it follows directly that

$$D(\tau_1) = -D(\tau_2) = -D(\sigma_2) = D(\sigma_1)$$

□

By combining the arguments in this section it follows that

Corollary 2.16. The complement of Σ consists of four connected components.

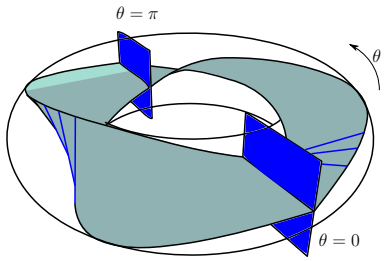

Figure 7: An artistic illustration of the θ-sections of a special linear robot. At $\theta = 0$ and $\theta = \pi$ the singularities are the whole xy-plane. At the other θ-sections the singularity set is a (blue) line on the "twisted strip". The singularity-free region can be thought of as the complement of the twisted strip and the two planes in the torus.

3. 3-RPR Triangle-Line Planar Platforms

Consider now a 3-RPR planar parallel robot with one (fixed) linear platform and a (moving) triangular platform for which the anchor points are distinct. In this section we will refer to it shortly as *hybrid robot* and we focus on *general* ones, i.e. $f_3 m_2 \neq m_3$. We make similar assumptions as in the linear robots but now $M_3 = (m_3, n_3)$.

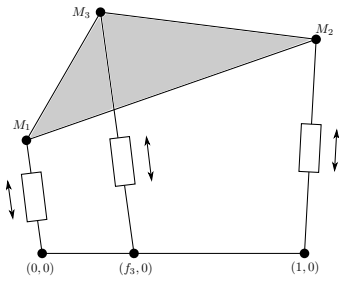

Figure 8: An illustration of a hybrid robot. The design parameters f_3, m_2, m_3, n_3 can take any value in $\mathbb{R}$ as long as the anchor points remain distinct.

Using similar notations as in Section 2, the kinematic map $F : \mathrm{SE}(2) \to \mathbb{R}^3$, of the robot is

$$F(\theta, x, y) := (x^2 + y^2, (m_2 c - 1 + x)^2 + (m_2 s + y)^2, (m_3 c - n_3 s - f_3 + x)^2 + (m_3 s + n_3 c + y)^2)$$

The set of singularities Σ is defined by the zero set of the determinant of the Jacobian of the kinematic map $D(c, s, x, y)$ in $\mathrm{SE}(2)$, where $c = \cos\theta$ and $s = \sin\theta$ for $\theta \in [0, 2\pi)$.

For all but finitely many θ-sections, D defines a hyperbola in the xy-plane. In this case one can continuously displace the singularity sets in every θ-section and express the equation of the hyperbolas in normal form, given by

$$A(\theta)x^2 - B(\theta)y^2 = 2f_3 m_2 (f_3 - 1)C(\theta)s \tag{4}$$

where

$$A(\theta) := (f_3 m_2 - m_3)c + n_3 s - \sqrt{(f_3 m_2 - m_3)^2 + n_3^2}$$
$$B(\theta) := (f_3 m_2 - m_3)c + n_3 s + \sqrt{(f_3 m_2 - m_3)^2 + n_3^2}$$

and where $C(\theta) := \frac{d_1 d_2 d_3}{d_0^2}$ with

$$d_0(\theta) := n_3 c - (f_3 m_2 - m_3)s$$
$$d_1(\theta) := n_3 c + m_3 s$$
$$d_2(\theta) := n_3 c + (m_3 - m_2)s$$
$$d_3(\theta) := n_3 c - (f_3 m_2 - m_3)s - m_2 n_3$$

Now the same methods as in the previous section (i.e. by continuously tracking θ-sections) can be applied to prove the following (the figures below describes the idea of the proof).

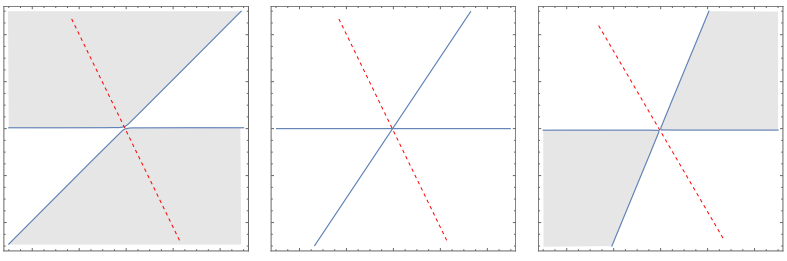

Figure 9: The red dashed line is one of the principal axes we continuously follow. Filled regions are the interiors of each hyperbola.

Theorem 3.1. The complement of Σ consists of two connected components.

Proof. At those finitely many θ-sections for which D does not define a hyperbola, we have either two intersecting lines or a parabola. The intersecting lines intersect at a point that is a pinch point of the surface Σ, while the transition to a parabola section can be regarded as the shrinking away of a branch of the hyperbola. Therefore it suffices to prove that there is a path from inside of a branch of a hyperbola at any θ-section to the inside of the opposing branch of the same θ-section. In fact, we will prove that as we continuously follow the θ-sections within a small interval of θ, the branches of the associated hyperbola degenerate and regenerate while the principal axes switch

roles i.e. a principal axis transforms from transverse axis to a non-transverse axis (and vice versa). This implies that the two branches open up and this allows a passage between them.

For a θ, the hyperbola has principal axes whose angle ϕ with the x-axis is given by

$$\tan 2\phi = \frac{(f_3 m_2 - m_3)s - n_3 c}{(f_3 m_2 - m_3)c + n_3 s} \tag{5}$$

We follow one solution branch $\phi_1(\theta)$ of (5) and displace the associated hyperbola by moving the center to the origin and rotating by ϕ_1 such that the new hyperbola is in normal form, as in (4).

For a general hybrid robot, we can obtain a small interval centred at 0 such that for any θ in there, $A(\theta), B(\theta)$ and $C(\theta)$ do not change signs, whilst within the same interval, $\sin(\theta)$ takes negative and positive values. This implies that the principal axis that we track with ϕ_1 jumps from being a transverse axis to a non-transverse axis (or vice-versa) and this is illustrated in Figure 9.

Thereby, we can move from the inside of one branch of a hyperbola in a θ-section to the inside of the other branch of the same θ-section by crossing $\theta = 0$. □

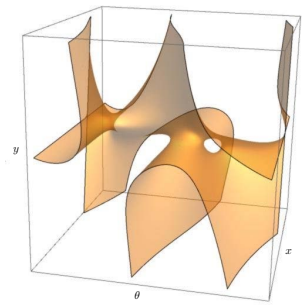

Figure 10: A plot of Σ centred at $(\theta, x, y) = (0, 0, 0)$ where θ varies from $-\pi$ to π for a hybrid robot with design parameters $f_3 = 2, m_2 = 3, m_3 = 5, n_3 = 7$.

4. 3-RPR Triangular Planar Platforms

In this last section, we consider the most general and well-studied 3-RPR planar parallel robot, the one with two triangular platforms, which we call *triangular robot*. We make similar assumptions as in the other two robots. Specifically note that the anchor points of the fixed platform are $(0, 0), (1, 0), (f_3, g_3)$ and at zero-position these anchor points are connected respectively, by an RPR leg to the anchor points $M_1 = (0, 0), M_2 = (m_2, 0), M_3 = (m_3, n_3)$ of the moving platform.

4.1. General Case

Throughout this section, when we write *general* robot we mean the one just described when the two triangles are not similar, i.e. when $f_3 m_2 \neq m_3$ or $g_3 m_2 \neq n_3$. Before we prove that the singularity-free space of this robot consists of two connected components, we will comment on how this was proven in the past.

Remark 4.1. It was first mentioned in [9] that the connected components of the singularity-free space of a general triangular robot are two. Husty shows that the number of connected components of the complement of the singularity surface Σ is equal to the number of connected components of the complement of another surface Σ' in $\mathbb{P}^3(\mathbb{R})$ (the image of Σ under a map defined by Blaschke and Grünwald) that is birational to Σ. The advantage of using Σ', is that Σ' is a smooth and compact real surface in $\mathbb{P}^3(\mathbb{R})$ (a sketch of the proof is given in [9]) and the number of connected components of the complement of Σ' is a result of the Jordan-Brouwer separation theorem [15].

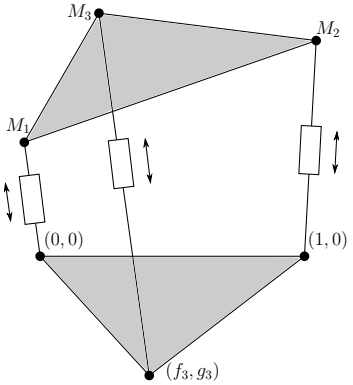

Figure 11: An illustration of a triangular robot. The design parameters f_3, g_3, m_2, m_3, n_3 can take any value in $\mathbb{R}$ as long as the anchor points remain distinct.

In [3], Coste provides an alternative proof and similarly suggests at investigating a modified kinematic surface Σ'' instead of Σ. Coste calls the product of the Möbius strip (without boundaries) and the real line, the *modified workspace* and argues that there is a natural map from the modified workspace to SE(2). The modified kinematic surface Σ'' is the preimage of Σ by this natural map. There is also a natural projection from the modified workspace to a torus and this is a line bundle. Coste then investigates the fibers of this line bundle with Σ'' to show that the complement of Σ'' is composed of two connected components.

In our proof, we will not need to modify the workspace or the singularity surface Σ. This gives us the advantage to fully understand the topology of Σ and its singularities. In fact, it is evident from the proof of Theorem 4.2 that the singularities of Σ are only finite number of pinch points.

The kinematic map $F : \mathrm{SE}(2) \to \mathbb{R}^3$, of the robot is (with the same notations as in Section 2)

$$F(\theta, x, y) := (x^2 + y^2, (m_2c - 1 + x)^2 + (m_2s + y)^2, (m_3c - n_3s - f_3 + x)^2 + (m_3s + n_3c - g_3 + y)^2)$$

The set of singularities Σ is defined by the zero set of the determinant of the Jacobian of the kinematic map $D(c, s, x, y)$ in SE(2), where $c = \cos\theta$ and $s = \sin\theta$ for $\theta \in [0, 2\pi)$.

For a fixed θ, D defines a conic in the xy-plane. This conic is a hyperbola or an ellipse, for all but finitely many θ-sections. The conics can degenerate at most in eight θ-sections and there are four or no θ-sections for which they are parabolas. This will be illustrated in the proof of 4.2.

For hyperbolas and ellipses we can continuously displace the θ-sections and get conics given by the following normal form

$$A(\theta)x^2 - B(\theta)y^2 = 2m_2C(\theta)s \tag{6}$$

where

$$A(\theta) := (f_3m_2 - m_3)c + (g_3m_2 + n_3)s - \sqrt{(f_3m_2 - m_3)^2 + (g_3m_2 - n_3)^2}$$
$$B(\theta) := (f_3m_2 - m_3)c + (g_3m_2 + n_3)s + \sqrt{(f_3m_2 - m_3)^2 + (g_3m_2 - n_3)^2}$$

and where $C(\theta) := \frac{d_1d_2d_3}{d_0}$ with

$$d_0(\theta) := 4g_3m_2n_3 - ((f_3m_2 - m_3)s - (g_3m_2 + n_3)c)^2$$
$$d_1(\theta) := (f_3n_3 - g_3m_3)c + (f_3m_3 + g_3n_3)s$$
$$d_2(\theta) := (f_3n_3 - g_3m_3 + g_3m_2 - n_3)c + (f_3m_3 + g_3n_3 - f_3m_2 + m_2 - m_3)s$$
$$d_3(\theta) := (f_3m_2 - m_3)s - (g_3m_2 + n_3)c + (m_2n_3 + g_3)$$

where the discriminant is d_0.

Theorem 4.2. The complement of Σ consists of two connected components.

Proof. Note that (as in Theorem 3.1) two of the θ-sections of Σ (i.e. $\theta = 0$ and $\theta = \pi$) are definitely those for which we have degenerate conics.

The discriminant tells us that if $g_3 m_2 n_3 < 0$, then all but finitely many θ-sections of Σ are hyperbolas. So we can use exactly the same argument as in the proof of Theorem 3.1 to prove that the complement of Σ consists of two connected components.

If $g_3 m_2 n_3 > 0$, we may have θ-sections of Σ that are ellipses. For the general case, we cannot just have ellipses (but even if we did, it is evident that we have only two connected components in the complement of Σ). In fact, for the general case, the condition of having θ-sections that are ellipses depends on whether the lines defined by

$$(f_3 m_2 - m_3)s - (g_3 m_2 + n_3)c \pm \sqrt{4 g_3 m_2 n_3}$$

intersect S^1 in the cs-plane. Clearly, these two lines are parallel and equidistant to the origin and the points were they intersect S^1 determine when the θ-section is a parabola. So we can have four or no θ-sections that are parabolas. If we only have hyperbola sections (i.e. the lines do not intersect the unit circle) then we are done, as we can use the proof of Theorem 3.1. If we have θ-sections that are ellipses, then for a general robot we will have infinitely many such θ-sections. In this case, the two lines cut S^1 in four arcs (see Figure 12). Two of the arcs contain $(1, 0)$ and $(-1, 0)$ and the θ-sections of Σ associated to the points on these arcs are hyperbolas (up to finitely many degenerations). The θ-sections of Σ associated to points on the other two arcs are ellipses.

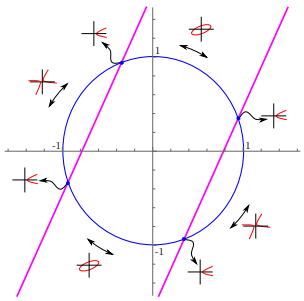

Figure 12: At $\theta = 0$ (the point $(1, 0)$) and $\theta = \pi$ (the point $(-1, 0)$) the θ-sections of Σ are two intersecting lines instead of a regular conic (hyperbola).

As we continuously follow a θ-section that is an ellipse to a θ-section that is a hyperbola, we can connect the interior of the ellipse with the interior of one of the branches of the hyperbola. We can do the same for the exteriors. So we only need to prove that we can find a path from the interior of one of the branches of the hyperbola to the interior of the other branch of a given θ-section without crossing Σ. We can now use the arguments of the proof of Theorem 3.1 in the neighborhoods of $\theta = 0$ and $\theta = \pi$ to conclude that this is possible. □

4.2. Special Case : Similar Triangles

Lastly we investigate the number of connected components of the singularity-free space of a robot with similar triangular platforms, where one is not the reflection of the other. The similarity condition translates in terms of design parameters to $f_3 m_2 = m_3$ and $g_3 m_2 = n_3$. One can easily compute that the determinant of the Jacobian of the kinematic map in this case is $D(c, s, x, y) = sg(c, s, x, y)$ where g is a quadratic polynomial in x and y. Thus, for $\theta = 0$ and $\theta = \pi$, the singularities are the whole xy-plane. Additionally the discriminant is $4n_3^3 s^2$, and the singularities is a circle in any θ-section when $\theta \neq 0$ and $\theta \neq \pi$. A degenerate θ-section occurs when $((c - m_2)^2 + s^2)s^3 = 0$, hence the only degenerate θ-sections would be when $s = 0$.

Proposition 4.3. The complement of Σ consists of four connected components.

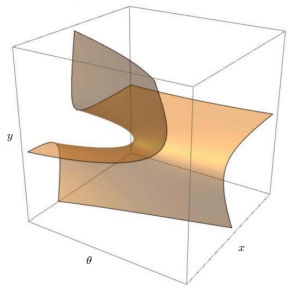

Figure 13: A local plot of Σ centred at $(\theta, x, y) = (0, 0, 0)$ for a general triangular robot with design parameters $f_3 = 2, m_2 = 3, m_3 = 5, n_3 = 7, g_3 = \frac{1}{3}$. The switch of the roles of the principal axes around $(0, 0, 0)$ is illustrated.

Proof. Since every θ-section with $\theta \neq 0$ and $\theta \neq \pi$ is non-degenerate, one can continuously follow the θ-sections for $\theta \in (0, \pi)$ and conclude that the singularity-free space consists of two connected components, one that is produced by the interiors of the circles and one by the exteriors. The same argument holds for $\theta \in (\pi, 2\pi)$, where we identify 2π with 0 in S^1. But the interior component for all $\theta \in (0, \pi)$ cannot be connected to the one for all $\theta \in (\pi, 2\pi)$ without crossing singularities, since for $\theta = 0$ and $\theta = \pi$ they are the whole xy-plane. The same holds for the exterior component. Thus the singularity-free space consists of exactly four connected components. □

Remark 4.4. Even if the triangles are congruent, i.e. $m_2 = \pm 1$, the only degenerate θ-sections would be when $s = 0$. Hence the number of connected components of the singularity-free space remains the same.

Acknowledgement

Both authors are supported by the joint French and Austrian ECARP project: ANR-19-CE48-0015, FWF I4452-N. The authors would also like to thank D. Salunkhe, P. Wenger and D. Chablat for their constructive discussions and comments.

References

[1] **M. Barton, N. Shragai, G. Elber** *Kinematic simulation of planar and spatial mechanisms using a polynomial constraints solver*, Computer-aided Design and Applications, Vol. 6, No. 1, pp. 115–123 (2009).

[2] **J. Capco, C. Spartalis**, *Code: Planar 3-RPR Parallel Robots with Linear Platforms (Maple and Mathematica Scripts)*, Zenodo (2021), https://doi.org/10.5281/zenodo.5046001

[3] **M. Coste**, *A Simple Proof That Generic 3-RPR Manipulators Have Two Aspects*, Journal of Mechanisms and Robotics. Vol 4, No. 1, pp. 011008-1–011008-6 (2012).

[4] **M. Coste, S. Moussa**, *Rationality of the Locus of Singularities of the General Gough–Stewart Platform*, SIAM Journal on Applied Algebra and Geometry, Vol. 4, No. 3, pp. 401–421 (2020).

[5] **M. Coste, S. Moussa**, *On the rationality of the singularity locus of a Gough-Stewart platform - biplanar case*, Mechanism and Machine Theory, Vol. 87, pp. 82–92 (2015).

[6] **M. Coste, P. Wenger, D. Chablat**, *Hidden Cusps*, Advances in Robot Kinematics, Proceedings in Advanced Robotics, Vol 4, pp. 129–138 (2016).

[7] **T. Fujita**, *Classification of Polarized Manifolds of Sectional Genus Two*, Algebraic Geometry and Commutative Algebra, pp. 73–98 (1988).

[8] **C. Gosselin, J.-P. Merlet**, *On the direct kinematics of planar parallel manipulators: special architectures and number of solutions*, Mechanism and Machine Theory, Vol. 29, No. 8, pp. 1083–1097 (1994).

[9] **M. Husty**, *Non-singular assembly mode change in 3-RPR parallel manipulators*, Proceedings of the 5th International Workshop on Computational Kinematics, pp. 51–60 (2009).

[10] **M. Husty, C. Gosselin**, *On the Singularity Surface of Planar 3-RPR Parallel Mechanisms*, Mechanics Based Design of Structures and Machines, Vol. 36, No. 4, pp. 411–425 (2008).

[11] **C. Innocenti, V. Parenti-Castelli**, *Singularity-free evolution from one configuration to another in serial and fully-parallel manipulators*, Journal of Mechanical Design, Vol. 120, No. 1, pp. 73–79 (1998).

[12] **A. Karger, M. Husty**, *Classification of all self-motions of the original Stewart-Gough Platform*, Computer-Aided Design, Vol. 30, No. 3, pp. 205–215 (1998).

[13] **X. Kong, C. Gosselin**, *Forward displacement analysis of third-class analytic 3-RPR planar parallel manipulators*, Mechanism and Machine Theory, Vol. 36, No. 9, pp. 1009–1018 (2001).
[14] **A. Lanteri, M. Palleschi, A.J. Sommese**, *Del Pezzo surfaces as hyperplane sections*, Journal of the Mathematical Society of Japan, Vol. 49, No. 3, pp. 501–529 (1997).
[15] **E.L. Lima**, *The Jordan-Brouwer Separation Theorem for Smooth Hypersurfaces*, American Mathematical Monthly, Vol. 95, No. 1, pp 39–42 (1988).
[16] **J.-P. Merlet**, *On the Separability of the Solutions of the Direct Kinematics of a Special Class of Planar 3-RPR Parallel Manipulator*, Proceedings of Design Engineering Technical Conferences, Vol. 4, pp. 457–462 (2000).
[17] **J.-P. Merlet**, *Parallel Robots*, 2nd. Edition, Springer, (2006).
[18] **D. H. Salunkhe, C. Spartalis, J. Capco, D. Chablat, P. Wenger**, *Necessary and sufficient condition for a generic 3R serial manipulator to be cuspidal*, Mechanism and Machine Theory, Vol. 171, 104729 (2022).
[19] **C. Wampler**, *Forward Displacement Analysis of General Six-In-Parallel SPS (Stewart) Platform Manipulators Using Soma Coordinates*, Mechanism and Machine Theory, Vol. 31, No. 3, pp. 331–337 (1996).
[20] **C. Wampler, A. Morgan, A. Sommese** *Numerical Continuation Methods for Solving Polynomial Systems Arising in Kinematics*, Journal of Mechanical Design, Vol. 112, No. 1, pp. 59–68 (1990).
[21] **P. Wenger**, *Cuspidal Robots*, Singular Configurations of Mechanisms and Manipulators, CISM International Centre of Mechanical Sciences, Vol. 589, pp. 67–99 (2019).
[22] **P. Wenger, D. Chablat, M. Zein**, *Degeneracy study of the forward kinematics of planar 3-RPR parallel manipulators*, Journal of Mechanical Design, Vol. 129, No. 12, pp. 1265–1268 (2007).